Front. Phys. China (2006) 4: 490－494
DOI 10.1007/s11467-006-0043-7

RESEARCH ARTICLE

ZENG Lei, JIN Feng-tao, YUAN Jian-min

Multipole effects to the opacity of hot dense gold plasma

Abstract The contributions of the multipole transitions to the opacity of hot dense gold plasma are taken into account by using an average-atom model. The influences of the E2, E3 and E4 transitions on the Rosseland opacity are studied, respectively. Comparisons with Miao's calculation have been made. It shows that using the Taylor series to account for the multipole transitions is no longer valid since i$\boldsymbol{k}\cdot\boldsymbol{r}$ is not much smaller than the unit when the photon energy goes very high.

Keywords plasma, opacity, multipole effects

PACS numbers 52.25.Os, 52.20.-j

1 Introduction

Generally, the magnitudes of the so-called higher order transitions, such as the magnetic dipole (M1) and the electric quadrupole (E2), are five to eight orders less than the electric dipole (E1) transitions among the valence states of atoms or ions. However, in a very hot and dense plasma, the inner-shell radiative transitions play an important role for the radiative transfer. For these kinds of inner-shell processes, transitions due to the higher order interactions than the E1 term cannot be neglected. A detailed study on the multipole effects in photoionization cross sections of isolated atoms was carried out by Ron *et al*. [1] within the independent particle model. For photoionization processes caused by higher energy photons above keV, the cross sections due to the E2 transition are comparable to, or even larger than those of the E1 transitions. For many cases, the contributions of the bound-free processes to the total opacity of hot and dense matters are considerable. In the present study, average-atom model [2, 3] is used to display the changes of the opacity caused by E2 transitions. And the electron orbitals are obtained by a widely-used scheme of a full self-consistent Dirac-Slater model [3－9]. Since the average-atom model is a one-electron approximation, there is no M1 transition between different electron orbitals, though the M1 transitions between the states of an actual atom within one electronic configuration can give comparable cross sections and interference effects with the E2 processes. However, the neglect of the M1 transitions would not induce loss in the radiative absorptions for high photon energies.

ZENG Lei, JIN Feng-tao, YUAN Jian-min (✉)
Department of Physics, National University of Defense Technology, Changsha 410073, China
E-mail: jmyuan@nudt.edu.cn

Received August 12, 2006

2 Method of calculation

In our AA model, the influence of the environment on the atom is assumed to have spherical symmetry on average. The movement of an electron under the interactions of the nucleus and other electrons is approximated by a central-field, which is determined with the standard self-consistent calculation. In the central-field, the radial part of the Dirac equation has the form:

$$\varphi=\frac{1}{r}\begin{pmatrix}P_{nk}(r)\chi_{km}(\hat{r})\\ \mathrm{i}Q_{nk}(r)\chi_{-km}(\hat{r})\end{pmatrix} \tag{1}$$

where $P_{nk}(r)$ and $Q_{nk}(r)$ are respectively the large and small component of the radial wave functions, and $\chi_{km}(\hat{r})$ is the spinor spherical harmonics. The movement of an electron under the interactions of the nucleus and other electrons is approximated by a central-field, which is determined with the standard self-consistent calculation. In the central-field, the radial part of the Dirac equation has the form:

$$\begin{aligned}\left(\frac{\mathrm{d}}{\mathrm{d}r}+\frac{k}{r}\right)P_{nk}(r)&=-\frac{1}{c}\left[\varepsilon-2c^2-U(r)Q_{nk}(r)\right]\\ \left(\frac{\mathrm{d}}{\mathrm{d}r}-\frac{k}{r}\right)Q_{nk}(r)&=\frac{1}{c}\left[\varepsilon-2c^2-U(r)P_{nk}(r)\right]\end{aligned} \tag{2}$$

where ε is the electron energy. The self-consistent potential $U(r)$ is composed of the static part, the exchange part and the correlation part, i.e., $U(r) = U_s(r) + U_{ex}(r) + U_{corr}(r)$. In the calculation the radial wave functions satisfy the boundary conditions:

$$\begin{aligned} &P_{nk}(r) \xrightarrow{r\to 0} ar^{l+1} \\ &P_{nk}(r_b) = 0 \end{aligned} \tag{3}$$

for bound electrons, and

$$\left.\frac{\ln P_{nk}(r)}{\mathrm{d}r}\right|_{r=r_b} = 0 \tag{4}$$

for free electrons, where r_b is the radius of the atom sphere. The bound electron density is obtained according to

$$\rho_b(r) = \frac{1}{4\pi r^2}\sum_j b_j\left(p_j^2(r) + Q_j^2(r)\right) \tag{5}$$

where b_j is the occupation number of the state j. In the average-atom model, the occupation number b_j is determined by the Fermi-Dirac distribution:

$$b_j = \frac{2\,|\,\kappa_j\,|}{\exp[(\varepsilon_j - \mu)/T] + 1} \tag{6}$$

The free electron is considered much more simply with an assumption of the Thomas-Fermi treatment, and the local free electron density is calculated with a Fermi-Dirac distribution of the local free electrons in the plane wave momentum k space, which can be written as:

$$\rho_f(r) = \frac{1}{\pi^2}\int_{k_0(r)}^{\infty} \frac{k^2\mathrm{d}k}{\mathrm{e}^{(\sqrt{k^2c^2+c^4}-c^2-V(r)-\mu)/T}+1} \tag{7}$$

where $k_0(r) = \sqrt{[2U(r)c^2 + U(r)^2]}/c$ and μ is the so-called chemical potential. The total electron density is the sum of $\rho_b(r)$ and $\rho_f(r)$,

$$\rho(r) = \rho_b(r) + \rho_f(r) \tag{8}$$

The chemical potential μ is determined so that the electrical neutrality is satisfied

$$\int_0^{\infty} 4\pi r^2\rho(r)\mathrm{d}r = Z \tag{9}$$

where Z is the nuclear charge [3].

In hot dense plasmas, with the increase of the density, the space occupied by an atom decreases and some high excited electrons will no longer be bound electrons. Thus the wave functions of an atom in high density plasma will be much different from that of free atoms. The size effects on the electronic structures of atoms and ions are considerable and must be included in the calculations. For pure matter the average atomic size is taken to be

$$R_b = \left(\frac{3V_0}{4\pi}\right)^{1/3} \tag{10}$$

where V_0 is the average atomic volume.

Contributions to the opacity consists of four parts [10, 11]:

$$\begin{aligned} \kappa_\nu = &\frac{N_A}{A}\left[\sigma^{bb}(h\nu) + \sigma^{bf}(h\nu) + \sigma^{ff}(h\nu)\right] \\ &\cdot\left[1 - \exp\left(-\frac{h\nu}{k_B T}\right)\right] + \kappa_s \end{aligned} \tag{11}$$

where N_A is the Avogadro constant, A is the atomic weight, k_B is the Boltzmann constant. $\sigma^{bb}(h\nu)$ and $\sigma^{bf}(h\nu)$ are the bound-bound and bound-free absorption cross sections at the photon energy of $h\nu$, respectively. The free-free, $\sigma^{ff}(h\nu)$, contribution takes Kramers hydrogen-like approximation:

$$\sigma^{ff}(h\nu) = \frac{32\pi^{5/2}Z^{*3}N_{ion}}{3\sqrt{6}c(k_B T)^{1/2}(h\nu)^3}g_{ff}(h\nu) \tag{12}$$

where $g_{ff}(h\nu)$ is the Gaunt factor. The scattering term, κ_s, is approximated by using Thompson scattering cross section.

The bound-bound and bound-free absorption cross sections are calculated respectively by:

$$\begin{aligned} \sigma^{bb}(h\nu) = &\frac{\pi he^2}{n_e c}\sum_{i,f}(2j_i+1) \\ &\cdot p_i(1-p_f)f_{i\to f}(h\nu)\varphi_{i\to f}(h\nu) \end{aligned} \tag{13}$$

and

$$\sigma^{bf}(h\nu) = \frac{\pi he^2}{m_e c}\sum_i (2j_i+1)p_i\frac{\mathrm{d}f_{i\to\varepsilon}}{\mathrm{d}(h\nu)} \tag{14}$$

where $\varphi_{i\to f}(h\nu)$ is the line profile taken as the Gaussian function.

The transition probability is proportional to the square of the matrix element $\left|\left\langle\varphi_f\left|\exp(\mathrm{i}\boldsymbol{k}\cdot\boldsymbol{r})\alpha\cdot\varepsilon\right|\varphi_i\right\rangle\right|^2$, where k is the photon wave number, r is the atomic radius, α is the 4×4 Dirac matrix and ε is the polarization vector of the photon. When $\mathrm{i}\boldsymbol{k}\cdot\boldsymbol{r}$ is much smaller than the unit, the term $\mathrm{e}^{\mathrm{i}\boldsymbol{k}\cdot\boldsymbol{r}}$ can be expressed in the Taylor series:

$$\mathrm{e}^{\mathrm{i}\boldsymbol{k}\cdot\boldsymbol{r}} = 1 + \mathrm{i}\boldsymbol{k}\cdot\boldsymbol{r} + \frac{(\mathrm{i}\boldsymbol{k}\cdot\boldsymbol{r})^2}{2!} + \cdots, \quad \boldsymbol{k}\cdot\boldsymbol{r} \ll 1 \tag{15}$$

where the terms in the right side are corresponding to the E1, M1, E2 transitions *et al*. However, this expression is no longer valid when the photon energy is sufficiently high, that is to say $\mathrm{i}\boldsymbol{k}\cdot\boldsymbol{r}$ is not much smaller than the unit. Then, $\mathrm{e}^{\mathrm{i}\boldsymbol{k}\cdot\boldsymbol{r}}$ can be expanded in a series of the spherical Bessel functions [12]:

$$\begin{aligned} \mathrm{e}^{\mathrm{i}\boldsymbol{k}\cdot\boldsymbol{r}} = &\sum_{L=1}^{M}(i)^L\sqrt{2\pi(2L+1)} \\ &\cdot\frac{1}{k\sqrt{L(L+1)}}(\nabla\times\boldsymbol{L})j_L(kr)Y_{LM}(\theta,\ \varphi) \end{aligned} \tag{16}$$

and the electric multipole transition probabilities both for bound-bound and bound-free transitions are written as:

$$W_{i\to f}=\frac{4\pi\,(2L+1)}{L+1}\frac{e^2}{\hbar c}v\,|\,R_{i\to f}\,|_L^2\;B(i,f,L) \tag{17}$$

in which i and f correspond to the initial and final state of the transition, and

$$\begin{aligned}|\,R_{i\to f}\,|_L^2=\Big[\int_0^{r_b}\frac{\mathrm{d}r}{kr}\{&[P_i(r)Q_f(r)+P_f(r)Q_i(r)](\kappa_i-\kappa_f)krj_{L-1}(kr)\\&+[(P_i(r)Q_f(r)+P_f(r)Q_i(r))L(L+1)\\&-(\kappa_f-\kappa_i)(P_i(r)P_\varepsilon(r)+Q_i(r)Q_\varepsilon(r))L]j_L(kr)\}\Big]\end{aligned} \tag{18}$$

and

$$\begin{aligned}B\;(i,f,\;L)&=(2l_i+1)(2j_f+1)\\&\cdot\left|C_{l_i0L0}^{l_f0}\right|^2W^2\left(l_ij_i,l_fj_f;\;\frac{1}{2}L\right)\end{aligned} \tag{19}$$

where $\left|C_{l_i0L0}^{l_f0}\right|^2$ and $W^2\left(l_ij_i,\,l_fj_f;\,\frac{1}{2}L\right)$ are respectively the Clebsch-Gordan coefficient and Racah coefficient, $j_L(kr)$ is the spherical Bessel function, and k is the wave vector.

With the transition probability $W_{i\to f}$ the oscillator strength is defined as [13]:

$$\begin{aligned}f_{i\to f}(h\nu)&=\frac{m_ec^3}{8\pi^2e^2v^3}W_{i\to f}\\&=\frac{m_ec^2}{2\pi\hbar\nu^2}\frac{2L+1}{L+1}\,|\,R_{i\to f}\,|_L^2\;B(i,f,L)\end{aligned} \tag{20}$$

In practical applications, Rosseland and Planck mean opacity are usually required. They are respectively defined by:

$$\begin{aligned}\frac{1}{\kappa_{\mathrm{R}}}&=\int_0^\infty\frac{W_{\mathrm{R}}(u)\mathrm{d}u}{K_\nu}\\\kappa_{\mathrm{P}}&=\int_0^\infty K_\nu W_{\mathrm{P}}(u)\mathrm{d}u\end{aligned} \tag{21}$$

where $u=h\nu/kT$, W_{R} and W_{P} are the Rosseland and Planck weighting functions:

$$\begin{aligned}W_{\mathrm{R}}(u)&=\frac{15}{4\pi^4}\frac{u^4\mathrm{e}^{-u}}{(1-\mathrm{e}^{-u})^2}\\W_{\mathrm{P}}(u)&=\frac{15}{\pi^4}\frac{u^3\mathrm{e}^{-u}}{1-\mathrm{e}^{-u}}\end{aligned} \tag{22}$$

3 Results and discussions

Firstly, we calculated the opacities only including the multipole effects of the bound-bound transitions. Table 1 shows the Rosseland mean opacities of Au at a density of 96.405 g · cm^{-3} when the maximum ranks of the electric multipole transitions are considered, respectively. From this table one can easily see that the Rosseland mean opacities have a perceptible increase when E2 transitions are included in the calculations. However, the contributions of the E3 and E4 transitions to the opacity are negligible. Figure 1 shows the spectrally resolved opacity of Au at the temperature of 5000 eV and the density of 96.405 g · cm^{-3}, in which the multipole effects of bound-bound and bound-free transitions have both been taken into account. The absorptions above 2400 a.u. are from the photoexcitations and photoionizations of the 1s orbital, and the absorptions below are from the higher orbitals. With the increase of the photon energy, the E2 transitions have more contributions to the total opacities. From Eq. (21) and Eq. (22) we can find that the Rosseland mean opacity is mainly determined by the bottom of the spectrum and the contributions from photoionizations become more important with the increase of the temperatures. For comparison, Miao's calculation [3] of Au plasma at the same conditions using the average atom model is plotted in Fig.2, in which the E2 transitions have been included. Unlike the present work, Miao *et al*. uses the first two terms in the Taylor series, i.e., Eq. (15), to account for the E1 and E2 transitions. In this figure one can see that the bound-free absorption has weak wiggles with the E2 transitions when the photon energy goes higher and higher. In the average atom model these kind of wiggles are due to the treatment of the electron radial wave functions in the plasma environment. In contrast to the E1 transition, such oscillations are more obvious for E2 transition due to the r^2 factor in the transition matrix rather than the r factor in E1 transition. However, such wiggles do not appear in Fig.1 because the present work expand i$\boldsymbol{k}\cdot\boldsymbol{r}$ using the spherical Bessel functions.

Table 1 Rosseland mean opacity of Au plasma at a density of 96.405 g · cm^{-3} when the maximum ranks of the electric multipole transitions are considered. κ_1, κ_2, κ_3, κ_4 refer the Rosseland mean opacities, in which up to E1, E2, E3, E4 transitions are considered, respectively.

T/eV	κ_1	κ_2	κ_3	κ_4
1000	270.17	270.50	270.50	270.50
2000	81.212	82.016	82.017	82.017
3000	45.921	46.255	46.257	46.257
4000	20.983	21.053	21.053	21.053
5000	7.622 4	7.640 7	7.640 8	7.640 8
6000	3.038 8	3.037 5	3.037 5	3.037 6
7000	1.471 3	1.472 5	1.472 5	1.472 5
8000	0.842 2	0.842 73	0.842 74	0.842 74
9000	0.591 44	0.591 74	0.591 74	0.591 74
10000	0.480 80	0.481 04	0.481 04	0.481 04

From Eq. (21), we know that the Rosseland mean opacity is sensitive to the bottom of the spectrum and the Rosseland weighting function reaches its maximum at 3.83 times the temperature. Thus one can expect that the bound-free absorptions would have main contributions to the Rosseland mean opacity when the temperature goes higher and higher. In Fig. 3, the Rosseland mean opacities of Au at the density of 96.405 g · cm^{-3} and temperatures from 1000—10 000 eV are plotted. It is obvious that the multipole effects become im-

portant only at the temperatures greater than 5 000 eV. In fact, at the temperature of 1000 eV there is only a 0.78 % difference between the Rosseland mean opacities with and without E2 and E3 transitions in the calculation. As the temperature increases to 10 000 eV, the relative difference between the Rosseland mean opacity with E2 and E3 transitions increases to 4.7 %. From Fig. 3 we can also see that the E3 transitions have little effect to the opacities at the temperatures having been studied. E3 transitions only have 0.007 % contributions to the total Rosseland mean opacity at a temperature of 1000 eV and increases to 1.7 % at a temperature of 10 000 eV. Consequently, the line with E2 transitions in Fig. 3 is almost overlapped by the line with E3 transitions. In the work of Miao *et al*., the contributions of E2 transitions only have 1.7 % difference to the total Rosseland mean opacity at a temperature of 1000 eV but increases to 85 % [3] at a temperature of 10000 eV. We think that this work has overestimated the contributions of the multipole effects since the Taylor series is no longer valid when the photon energy is very high and $i\boldsymbol{k}\cdot\boldsymbol{r}$ is therefore not smaller than the unit.

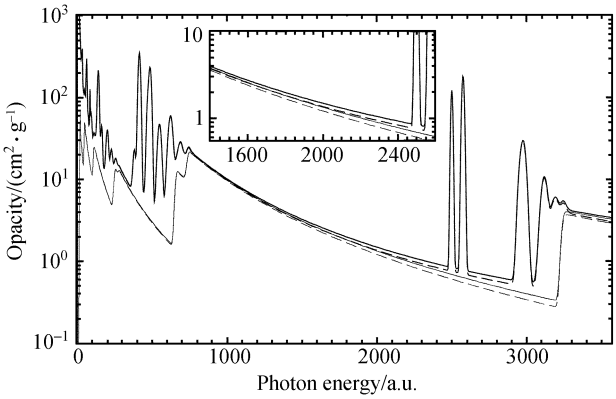

Fig. 1 The opacity of Au at T = 5000 eV and ρ = 96.405 g · cm^{-3}. The thick dashed and solid lines refer to the cases with and without E2 transitions considered, respectively. The thin dashed and solid lines refer to the bound-free opacity with and without E2 transition considered, respectively.

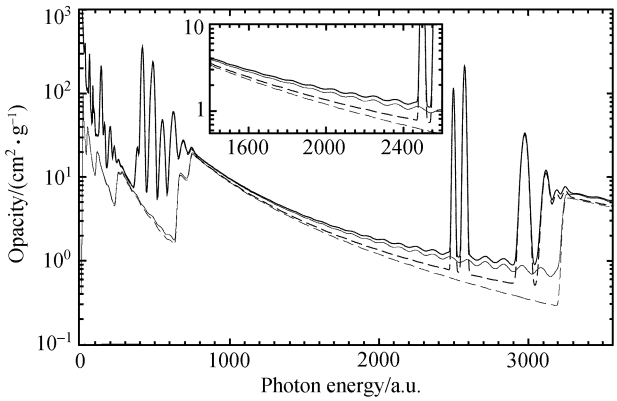

Fig. 2 Spectrally resolved opacity of Au Calculated by Miao *et al*. [3] at a temperature of 5000 eV and a density of 96.405 g · cm^{-3}. The long dashed line refers to the result of including E1 transition only. The long solid line refers to the result of including E1 and E2 transitions. The shot dashed line refers to the bf opacity including E1 transition only, and the shot solid line refers to result of including E1 and E2 transitions.

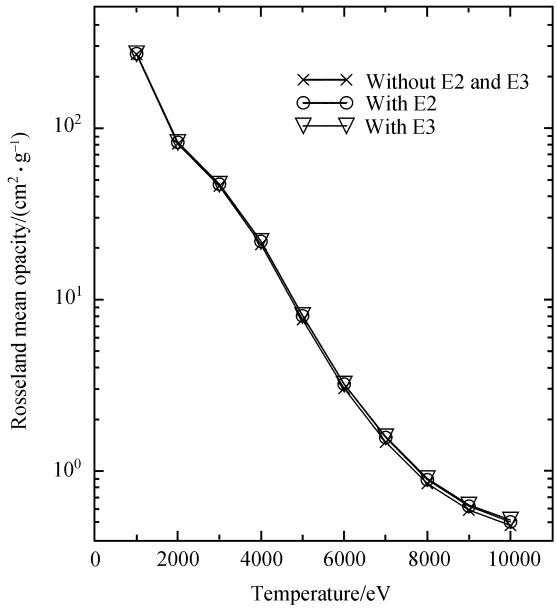

Fig. 3 Rosseland mean opacity versus temperature of Au at a density of 96.405 g · cm^{-3}.

In summary, we have studied the multipole effects to the opacities of hot gold plasmas using the average atom model. It shows that at higher temperatures the E2 transition has contributions to both the spectrally resolved opacity and the Rosseland mean opacity, but the contributions from E3 and E4 transitions are very small. Comparisons with the results obtained by Miao *et al*. show that the contributions of E2 transitions may be overestimated by the approaches of the Taylor series since $i\boldsymbol{k}\cdot\boldsymbol{r} \ll 1$ is not valid at very high photon energy.

Acknowledgements This work was supported by the National Science Fund for Distinguished Young Scholars under Grant No. 10025416, the National Natural Science Foundation of China under Grant No. 19974075 and 10204024, the National High-Tech ICF Committee in China, and the China Research Association of Atomic and Molecular Data.

References

1. Ron A., Goldberg I. B., Stein J., Manson S. T., Pratt R. H., and Yin R. Y., Relativistic, retardation, and multipole effects in photoionization cross sections: *Z*, *n*, and *l* dependence, Phys. Rev. A, 1994, 50: 1312
2. Yuan J. M., Self-consistent average-atom scheme for electronic structure of hot and dense plasmas of mixture, Phys. Rev. E, 2002, 66: 047401
3. Miao J. S. and Yuan J. M., Contribution of the E2 transitions to the opacity of hot and dense plasmas of heavy elements by an average-atom approach, Phys. Rev. E, 2004, 69: 017401
4. Rozsnyai B. F., Relativistic Hartree-Fock-Slater calculations for arbitrary temperature and matter density, Phys. Rev. A, 1972, 5: 1137
5. Faussurier G., Blancard C., and Decoster A., Statistical mechanics of highly charged ion plasmas in local thermodynamic equilibrium, Phys. Rev.E, 1997, 56:3474

6. Faussurier G., Blancard C., and Decoster A., Statistical treatment of radiative transitions in local thermodynamic equilibrium plasmas, Phys. Rev. E, 1997, 56: 3488
7. Wu Z. Q., Han G. X., and Peng J. Q., Opacity calculations for non-local thermodynamic equilibrium mixtures, Chin. Phys. Lett., 2002, 19: 518
8. Sun Y. S., Meng X. J., and Zheng S. T., Opacity calculation based on average atom model, Nuclear Science and Techniques, 1997, 8: 6
9. Zhao Y. J. and Zhang Z. J., Calculation of Atomic Structure. Beijing: Science Press, 1987 (in Chinese)
10. Zeng J. L., Study on the radiative opacity of aluminum plasmas using a model based on the detailed term accounting approximation, Changsha: National University of Defense Technology Press, 2005 (in Chinese)
11. Sun Y. S., Yuan J. K., and Zheng S. T., Radiative opacity for high Z elements, Chinese Journal of Computational Physics, 1997, 14:765
12. Scofield J. M., Radiative decay rates of vacancies in the K and L shells, Phys. Rev., 1969, 179: 9
13. Li S. C., Theory of hot radiation and quantum radiation. Beijing: National Defence Industry Press, 1992 (in Chinese)